Alexandria Engineering Journal 95 (2024) 101–113

Contents lists available at ScienceDirect

Alexandria Engineering Journal

journal homepage: www.elsevier.com/locate/aej

Original article

The removal of methylene blue from aqueous solutions by polyethylene microplastics: Modeling batch adsorption using random forest regression

Mehdi Bahrami [a,1], Mohammad Javad Amiri [a,1], Sara Rajabi [a], Mohamadreza Mahmoudi [b,*]

[a] Department of Water Engineering, Faculty of Agriculture, Fasa University, Fasa 74616-86131, Iran
[b] Department of Statistics, Faculty of Science, Fasa University, Fasa 74616-86131, Iran

ARTICLE INFO

Keywords:
Batch adsorption
Methylene blue
Microplastics
Random Forest regression

ABSTRACT

In light of the extensive contamination of water sources by microplastics, their substantial specific surface area makes them favorable candidates as adsorbents for the simultaneous removal of coexisting contaminants in wastewater. In this regard, polyethylene microplastics were utilized to eliminate methylene blue dye from water. MB adsorption onto microplastics reached equilibrium in just 30 min at pH 7. The better fit of fractional power and Redlich-Peterson models on kinetic and equilibrium adsorption data, respectively, revealed that the MB removal process is a chemisorption in multilayer adsorption on the heterogeneous surface of the microplastics particles. The reusability of the microplastics adsorbent was confirmed based on the promising outcomes observed after five cycles. The results of the random forest regression exhibited an R^2 of 97.55% for the correlation between the model-computed and measured amounts of MB reduction. The sensitivity analysis illustrated that the MB sorption process on microplastics is highly influenced by the initial MB concentration and adsorbent mass. These results show that although microplastics may pose potential risks to water environments, their adsorption potential can be utilized to simultaneously omit other pollutants from the aqueous solutions.

1. Introduction

The global effort to deal with environmental issues and ensure the sustainability of the environment around the world has increased daily [1–3]. The world is interconnected and integrated by technology, where issues in one-part affect other regions. One of these problems is the growth of industrial and agricultural activities, which have increased the entry of wastewater containing toxic contaminants into the environment [4]. The improper treatment of this wastewater leads to disastrous environmental consequences and threatens human society's health [5]. The Environmental Protection Agency (EPA) has classified dyes as a national secondary drinking water contaminant. Over 100,000 commercially available dyes are extensively used in various sectors, like textiles, pharmaceuticals, cosmetics, plastics, paper, leather, paint industries, and food processing. After usage, 700,000 tons of dyes are produced annually by these industries, of which 12–14 percent are discharged into the environment. Colored effluents may degrade soil quality, influence plant growth by disrupting photosynthetic action, and enhance the toxicity of water bodies [6]. Methylene blue (MB) is a stable, cheap, reactive, and highly colored cationic dye with a molecular formula of C16H18N3S(Cl) and a molecular weight of 319.85 g/mol, usually available as dark green crystals as a dye [7].

Physical [8,9], chemical [10], and biological processes [11] can reduce problems associated with dye contamination. Adsorption is among the most extensively employed techniques for removing dyes, especially non-degradable ones [12–16]. Nano and micro-structure adsorbents with high specific surface area and exceptional adsorption capability [17–19], in addition to the high efficiency of adsorption processes, justify the use of this process from an economic standpoint, as it allows for the recovery and reuse of the adsorbent.[20].

Microplastics (MP), commonly characterized as plastic waste smaller than 5 mm, have been found in various environments, including lakes, estuaries, oceans, and even outlying locations like polar regions [21]. Given that wastewater treatment plants (WWTPs) are not specially prepared for MP disposal, however, MP elimination appears to happen with high performance, and millions of MP are discharged from WWTPs to the receiving environment in a day [22,23]. These effluents involve MP with contaminants like heavy metals, pesticides, antibiotics, polyaromatic hydrocarbons (PAHs), polychlorinated biphenyls (PCBs), and bisphenols. Because of their extensive surface area, MPs attract

* Corresponding author.
E-mail address: mahmoudi.m.r@fasau.ac.ir (M. Mahmoudi).
[1] These authors contributed equally to this work.

https://doi.org/10.1016/j.aej.2024.03.100
Received 1 October 2023; Received in revised form 20 February 2024; Accepted 26 March 2024
Available online 1 April 2024
1110-0168/© 2024 The Author(s). Published by Elsevier BV on behalf of Faculty of Engineering, Alexandria University This is an open access article under the CC BY-NC-ND license (http://creativecommons.org/licenses/by-nc-nd/4.0/).

contaminants in the effluent that causes a synergistic toxic impact on organisms in the receiving aquatic environment. In addition to the studies on microplastic removal from water sources [24,25], many researchers have used this ability to adsorb various coexisting pollutants by microplastics from aqueous solution [26–29]. Therefore, microplastics in aquatic environments near pollutant discharge points are important adsorbents in removing various contaminants such as arsenic [30], cadmium [31], lead [32], tetracycline hydrochloride [33], and MB [34]. Zhao et al. [35] reviewed the excellent potential of microplastics in sewage treatment. They concluded that, compared to other adsorbents, microplastics offer advantages such as high adsorption capacity, adsorption efficiency, and reusability in sewage refinement.

The utilization of polyethylene microplastics as adsorbents for water treatment represents a relatively new and emerging field of research. Polyethylene microplastics were employed in this research for MB removal due to several factors, including their low cost, high surface area-to-volume ratio, availability, and capability to be easily modified with chemical or physical treatments to enhance their adsorption capacity. Moreover, polyethylene microplastics are non-toxic and non-reactive, making them safe for use in wastewater treatment. Polyethylene microplastics offer the advantage of easy recyclability and reusability in adsorption processes, making them an environmentally friendly alternative compared to materials that may not be recyclable [36–38]. Although microplastics are a concern in terms of environmental pollution, repurposing them as adsorbents provides a promising solution for their management and utilization. Overall, the use of microplastics as adsorbents for water treatment offers several key benefits, including high adsorption capacity, cost-effectiveness, scalability, reusability potential, and the ability to remove persistent organic pollutants. However, it is crucial to implement proper risk assessment, management strategies, and regulatory oversight to ensure the safe and responsible use of microplastics in water treatment applications [39–41]. Alternatively, the efficiency of (MB) removal in water treatment processes can be influenced by the type (low-density polyethylene (LDPE) or high-density polyethylene (HDPE)) and size of polyethylene microplastics. Additionally, the smaller size of microplastics presents difficulties in their separation from treated water. Their diminutive dimensions increase the likelihood of bypassing filtration systems, which in turn can result in their potential release into the environment, posing risks to aquatic organisms

The parameters affecting the adsorption process in a volumetric system are pH, initial concentration of pollutant, contact time, adsorbent dose, and temperature, which have complex relations to adsorption capacity [42]. The successful development of artificial neural networks has enabled the prediction of target pollutants in aqueous media [43]. Regrettably, artificial neural networks models are often considered black-box methods, meaning their inner workings and rules are not easily interpretable. Utilizing these models can be challenging and may have a risk of overfitting. The determination of the optimal structure of these models typically relies on trial and error, a process that demands significant computational time. Moreover, the strong dependence of artificial neural networks models on experimental data poses a major challenge for these methods. Conversely, achieving reliable modeling of the adsorption process necessitates the utilization of appropriate numerical procedures [44]. However, these procedures may encounter convergence issues arising from inadequate initialization and the non-linearity inherent in the problem being solved. Alternatively, machine learning algorithm models have been proposed for data correlation in order to address this issue [45,46]. Researchers often choose random forest regression as a modeling method for the adsorption process due to its capabilities in handling non-linearity, robustness to outliers, handling high-dimensional data, feature importance, and ensemble learning. These features make random forest regression well-suited for capturing complex relationships, addressing data variability, managing multiple variables, identifying influential factors, and improving generalization performance in adsorption modeling studies

Therefore, because of the vast existence of microplastics in various water sources, in this research, we tried to use this threat as an opportunity to adsorb and remove the MB pollutant from the aqueous solution. The primary objectives of this study are: (1) to examine the polyethylene microplastics as a novel adsorbent to remove methylene blue dye from the aqueous solution, (2) to describe step-by-step the adsorption process of MB through the MP by utilizing BET, BJH, FT-IR, FE-SEM, and EDS, (3) to determine the kinetics, equilibrium isotherms, and thermodynamics parameters, and (4) to model the MB adsorption capacity by MP affected by operating parameters, including pH, temperature (Temp), contact time (time), pollutant concentration (C_0), and adsorbent dosage (C_s), by applying random forest regression technique.

2. Materials and methods

2.1. Chemicals and instruments

Analytical grade MB dye, purchased from Sigma Aldrich (Germany), was used as the pollutant. The polyethylene microplastic used in the study was prepared by the Department of Materials Science and Engineering at Shiraz University. Other chemicals, namely NaOH (99%) and HCL (37%), were sourced from Merck, Germany. The Brunnauer-Emmett-Teller (BET) technique was utilized to determine the specific surface area of the adsorbent, while the Barrett-Joyner-Halenda (BJH) method was employed to calculate the pore size. The Fourier transform infrared spectrometer (FT-IR) technique was applied to investigate the functional groups existing on microplastics. The size and morphology of the microplastic surface were determined using a field emission scanning electron microscope (FE-SEM), and the constituent elements of microplastic were identified using energy dispersive spectroscopy (EDS).

2.2. Adsorption tests

Batch experiments were carried out to determine the adsorption capacity and reusability of the microplastic adsorbent after desorption of methylene blue, as well as the changes in its effectiveness. To investigate the adsorption of MB by a microplastic adsorbent under various experimental conditions, MB stock solutions were obtained by dissolving a given mass of solute in distilled water, followed by dilution to reach the desired concentration. Then, 30 mL of this solution containing specified methylene blue pollutant concentration (C_0, 1–60 mg/L) was adjusted with 0.1 N HCl or NaOH on the desired pH value (2−10). After adding a specific amount of microplastic adsorbent (D_s, 0.1–1 g) to the solution, the container was agitated using a rotary orbital shaker SEBD001 operating at a speed of 120 rpm at room temperature (25 ± 2 °C). Once the desired contact time (time, 30–480 min) had elapsed, the mixture was filtered through Whatman filter paper, and the remaining concentration of MB in the solution was measured using a UV-Vis spectrophotometer at a wavelength of $\lambda_{max} = 664$ nm. Adsorption efficiency (R) and adsorption capacity at equilibrium (q_e, mg/g) and at any time (q_t, mg/g) of microplastics for removal of MB were calculated as:

$$R = \left(\frac{C_0 - C_e}{C_0}\right) \times 100 \quad (1)$$

$$q_e = \frac{(C_0 - C_e)V}{m} \quad (2)$$

$$q_t = \frac{(C_0 - C_t)V}{m} \quad (3)$$

where C_0, C_e, and C_t represent the initial MB concentration, MB concentration at equilibrium, and MB concentration at any given time (mg/L), while m and V represent the adsorbent mass (g) and the volume of the MB solution (L), respectively.

The kinetic equations were fitted to data from different contact times

(30, 60, 120, 240, 360, and 480 min) at the constant adsorbent dose of 0.1 g, MB initial concentration of 20 mg/L, and solution pH equal 7. The isotherm models were fitted to data from varying adsorbent doses (0.1, 0.3, 0.5, 0.7, and 1 g) at MB initial concentration of 20 mg/L, solution pH 7, and contact time of 30 min. Thermodynamic studies were also executed by setting the temperature in the incubator at three various temperatures (Temp, 40, 50, and 60 °C) at MB initial concentration 20 mg/L, adsorbent dose 0.1 g, time 30 min, and pH 7.

Following the adsorption process and separation of the adsorbent through filter paper, the microplastic adsorbent was agitated in a 30 mL solution of 0.1 M hydrochloric acid. The MB concentration in this solution was measured using a spectrophotometer, which indicates the quantity of desorbed dye from the adsorbent (q_d, mg/g). Then, the recovered microplastics were reused to adsorb MB from the aqueous solution (q_a, mg/g). The reusability experimentations were conducted using the same conditions as the adsorption process, which included an MB initial concentration of 20 mg/L, 1 g microplastic adsorbent, and a contact time of 30 min. The recycling operation was repeated five times to assess the efficiency of the microplastic adsorbent after each wash. Finally, the percentage of MB dye desorption (%Desorption) for each round was calculated as follows:

$$\%Desorption = \frac{q_d}{q_a} \times 100 \tag{4}$$

2.2.1. Adsorption kinetics

The kinetics models were estimated to designate the mechanism and rate of the adsorption process. This kinetics relies on the properties of the adsorbate, adsorbent, and experimental conditions. Various reaction kinetics models, including pseudo-first-order (PFO), pseudo-second-order (PSO), Elovic, and fractional power (F-P) equations were attempted to assess the reaction rate and mechanism of MB adsorption on microplastic surfaces [47,48].

The PFO model for the attraction of MB on microplastic was investigated using the following equation, which assumes that one adsorbate molecule is bound to one binding site of the adsorbent in the solid-liquid system:

$$q_t = q_e\left(1 - e^{-K_1 t}\right) \tag{5}$$

where q_e and q_t represent the quantity of material adsorbed per unit mass of the sorbent at equilibrium and time t (mg/g), respectively, and K_1 represents the rate constant of PFO's surface adsorption (1/min).

According to the pseudo-second-order kinetic model, the rate-limiting step is chemical sorption, and it can forecast the behavior of adsorption throughout the entire range:

$$q_t = \frac{K_2 q_e^2 t}{1 + K_2 q_e t} \tag{6}$$

where K_2 is the pseudo-second-order velocity constant (mg/g min).

The Elovich kinetic model, which is often applied for systems with heterogeneous surfaces and chemical adsorption kinetics, is also based on the adsorption capacity of the adsorbent, as noted by Low [49].

$$q_t = \left(\frac{1}{\beta}\right)\ln\left(\alpha\beta\right) + \left(\frac{1}{\beta}\right)\ln t \tag{7}$$

where α and β represent the initial adsorption rate constant (mg/g.min) and the desorption constant (g/mg), respectively.

The fractional power model can also be expressed in a non-linear form as follows:

$$q_t = at^b \tag{8}$$

where a represents the initial adsorption rate constant (mg/g), and b represents the adsorption rate coefficient (1/h).

2.2.2. Adsorption isotherms

The quantity of adsorbed molecules as a function of concentration at a constant temperature is described by adsorption equilibrium isotherms. The equilibrium characteristics of MB removal from aqueous solution were evaluated in this study using Langmuir, Freundlich, Temkin, and Redlich-Peterson (R-P) isotherm models, as documented by Xu et al. [47] and Saruchi [48].

The Langmuir model is the most fundamental theory for surface adsorption, postulating that adsorption takes place at homogeneous sites on the adsorbent in a monolayer. As per the Langmuir model, the adsorption site becomes saturated once occupied, making further adsorption impossible. Ultimately, the adsorbent surface attains a saturation point, which represents the maximum adsorption capacity of the surface.

$$q_e = \frac{bq_m C_e}{1 + bC_e} \tag{9}$$

where C_e represents the equilibrium concentration of the solution (mg/L), and q_e and q_m refer to the adsorption capacity in the equilibrium state and the maximum adsorption capacity (mg/g), respectively. Additionally, b denotes the Langmuir constant (L/mg), which indicates the adsorbate's affinity for adsorption on the adsorbent. q_m is used to evaluate the efficiency of adsorbents so that the q_m and b values should be high in a suitable adsorbent. Additionally, the R_L index can be employed to forecast the adsorption process:

$$R_L = \frac{1}{(1 + bC_0)} \tag{10}$$

This index aids in predicting the adsorption process so that $R_L>1$ is an undesirable adsorption process, $0<R_L<1$ is a favorable adsorption process, $R_L=1$ is a linear process, and $R_L=0$ shows an irreversible and inefficient process.

The Freundlich model is an empirical relationship that explores the multilayer adsorption process on heterogeneous adsorbent surfaces with sites of various affinities:

$$q_e = K_F C_e^{\frac{1}{n}} \tag{11}$$

where K_F represents adsorption capacity $(mg/g)(mg/L)^{-n}$ and n reflects model exponent (-), known as heterogeneity factor and is suggestive of the deviation from linearity of adsorption. A value of n equal to 1 indicates that the process is linear, while values greater than 1 suggest a physical adsorption process, and ones less than 1 offer a chemical adsorption process.

By examining the impact of adsorbate-adsorbent interactions on the exposure of the adsorbent surface, the Temkin isotherm demonstrates a linear decrease in the heat of adsorption of complete adsorbate molecules.

$$q_e = \frac{RT}{b_T}\ln A_T C_e \tag{12}$$

where A_T represents the equilibrium binding constant (L/g), b_T is related to the heat of adsorption (J/mol), T is the absolute temperature (K), and R is the gas constant equals 8.314 J/K.mol.

The Redlich-Peterson model is used for adsorption within a broad concentration range in homogeneous or heterogeneous systems depending on the conditions [50]. This isotherm model is characterized as follows:

$$q_e = \frac{aC_e}{1 + bC_e^n} \tag{13}$$

where a represents the solutes absorptivity (L/g), b is the Redlich-Peterson isotherm constant associated with the adsorption energy $(L/mg)^n$, and n is the power of the Redlich-Peterson equation ($0<n<1$).

2.2.3. Thermodynamic equations

The adsorption mechanism is investigated by thermodynamic parameters, including the change in standard enthalpy(ΔH°), standard entropy (ΔS°), and Gibbs standard free energy (ΔG°) for the adsorption process using Van't Hoff equations [51]:

$$K_d = \frac{q_e}{C_e} \tag{14}$$

$$K_c = 1000 K_d \tag{15}$$

$$\Delta G^{\circ} = -RT \ln K_c \tag{16}$$

$$\ln K_c = \frac{\Delta S^{\circ}}{R} - \frac{\Delta H^{\circ}}{RT} \tag{17}$$

where K_d represents the distribution coefficient of adsorbate (L/g), q_e denotes the quantity of MB adsorption in equilibrium (mg/g), C_e is the equilibrium concentration of MB in solution (mg/L), K_c is the ratio of MB removed by microplastic (mg/g) to the remained MB in the solution (mg/L), R is the global gas constant (8.314 J/K.mol), and T is the solution temperature (K).

2.3. Modeling the adsorption process

The robustness of the random forest regression model was estimated for the expression of MB removal from an aqueous environment by microplastic in batch experiments. Random forest is a classification algorithm that consists of a set of decision trees to minimize the variance of the output generated by each tree, leading to enhanced stability and precision in classification. Typically, the random forest technique is usually created based on two primary concepts: bagging and random selection [52]. Random Forest Regression is built upon several assumptions, including independence, linearity, homoscedasticity, normality, and multicollinearity. Random Forest assumes that the observations in the dataset are independent of each other. Random Forest, renowned for its capability to handle non-linear relationships, does not make the assumption of linearity between the predictors and the response variable. Random Forest Regression does not assume homoscedasticity, meaning that it does not require the residuals to have constant variance across different levels of the predictors. Unlike linear regression, Random Forest Regression does not assume that the residuals follow a normal distribution. Random Forest is capable of handling multicollinearity, which refers to the presence of high correlation between predictors [53,54]. In random forest regression, the bagging bootstrap aggregation approach is applied to produce numerous trees without any interactions. Then the model is run parallel and independently on each tree and finally the outputs of the trees are aggregated. In other words, the random forest combines multiple decision trees to determine the final output rather than relying on individual decision trees. For the current research, the input data for the random forest model were the parameters of pH, reaction time, adsorbent dosage, temperature, and initial concentration of MB, while the output was the MB adsorption capacity by MP. The model was evaluated using 25 sets of experimental data, with 70% of the data used for training and the remaining data for validation.

2.4. Evaluation criteria

To evaluate and compare these models to choose the best equation describing the removal of MB, mathematical error functions such as the coefficient of determination (R^2), root-mean-square error (RMSE), absolute relative error (ARE), the sum of absolute errors (SAE), the sum of squared errors (SSE), Marquardt standard deviation percentage (MPSD), and hybrid fractional error function (HYBRID) were determined in SPSS (Table 1) [55]. Finally, by using the non-parametric Friedman test, which is used to detect the difference between related data, the kinetic and isotherm models were ranked, and the best model was selected according to the lowest rank.

Table 1
Error functions used to compare models.

Criterion	Symbol	Formula
R-squared	R^2	$R^2 = \frac{\sum (q_{obs} - \overline{q}_{pre})^2}{\sum (q_{obs} - \overline{q}_{pre})^2 + \sum (q_{obs} - q_{pre})^2}$
Root-mean-square error	RMSE	$RMSE = \sqrt{\frac{\sum_{i=1}^{n} (q_{obs} - q_{pre})^2}{n}}$
Absolute relative error	ARE	$ARE = \frac{100}{n} \sum_{i=1}^{n} \left\lvert \frac{q_{obs} - q_{pre}}{q_{obs}} \right\rvert$
The sum of absolute errors	SAE	$SAE = \sum_{i=1}^{n} \left\lvert q_{obs} - q_{pre} \right\rvert_i^2$
The sum of squared error	SSE	$SSE = \sum_{i=1}^{n} (q_{obs} - q_{pre})_i^2$
Marquardt's percentage standard deviation	MPSD	$MPSD = 100 \sqrt{\frac{1}{n-p} \sum_{i=1}^{n} \left(\frac{q_{obs} - q_{pre}}{q_{obs}} \right)^2}$
HYBRID	HYBRID	$HYBRID = \frac{100}{n-p} \sum_{i=1}^{n} \left\lvert \frac{q_{obs} - q_{pre}}{q_{obs}} \right\rvert$

q_{obs} and q_{pre} are respectively measured and predicted adsorption capacity at time t, n denotes the number of observed values, and p represents the number of factors.

3. Results and discussion

3.1. Adsorbent characteristics

The FTIR spectrum of microplastic before and after MB adsorption is represented in Fig. 1. Before the adsorption of MB, the peak within the 3500–3400 cm^{-1} is related to hydroxyl groups (O-H), which allows the formation of hydrogen bonds [56]. The stretching vibration peak in the 3441 cm^{-1} spectra is attributed to the N-H bond in the amine group [57]. The 2840–3000 cm^{-1} band is associated with C-H aromatic bonds. The strong bands in the 1611.34 cm^{-1} and 2368.41 cm^{-1} are related to C═C and O═C═O stretching bonds, respectively [58]. The peak of 1460.07 cm^{-1} is attributed to the C-H bending bond. The 1264.72 cm^{-1} band indicates the existence of a strong C-O stretching bond. Also, the spectrum in the range of 54.720–996.07 cm^{-1} is allocated to the strong C═C bending bond. After MB absorption, the bands of 3441.48, 2927.25, 2368.41, 1611.34, and 467.36 cm^{-1} were transferred to 2920.30, 2634.83, 2021.33, 1466.42, and 720.49 cm^{-1} respectively, that the sharp peak at 720.49 cm^{-1} is indicative of the strong C═C bending bond. The peak in 48.3441 cm^{-1} has disappeared, and one in the range of 38.2851–30.2920 cm^{-1} has been added, related to the C-H stretching bond. Also, a peak in 1611.34 cm^{-1} has been lost. All these changes indicate the adsorption of MB by the microplastic adsorbent, which reflects minor changes in the molecular structure.

SEM images of microplastics shown in Fig. 2 indicate the non-porous microplastic structure owning holes, in which the shape of the holes is irregular and chaotic, and the shape and size distribution of the holes are unknown. Therefore, there is a possibility of adsorbing MB molecules between the holes by this adsorbent.

X-ray energy diffraction spectroscopy of microplastic (Fig. 3) revealed that the constituent elements include carbon, oxygen, copper, titanium, and calcium, whose weight percentages in the microplastic sample were 95.9%, 3.2%, 0.5%, 0.2%, and 0.2%, respectively.

The determination of the specific surface area of an adsorbent is frequently carried out using the BET (Brunauer, Emmett, and Teller) method, which is widely accepted as the standard technique. This model uses gases, which do not chemically react with the material surface but allow the adsorption of gas molecules to the solid surface, which

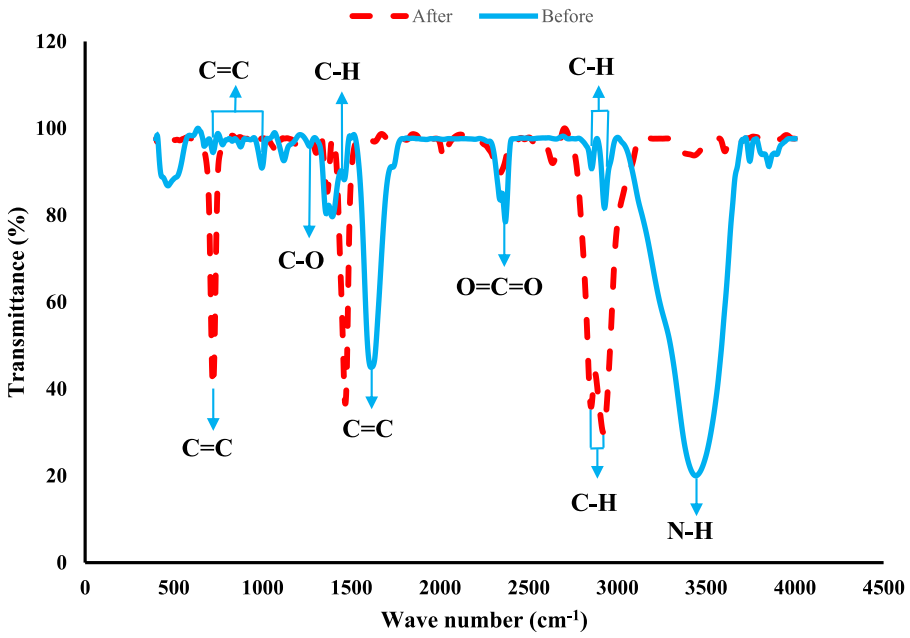

Fig. 1. FTIR spectrum of microplastic before and after MB adsorption.

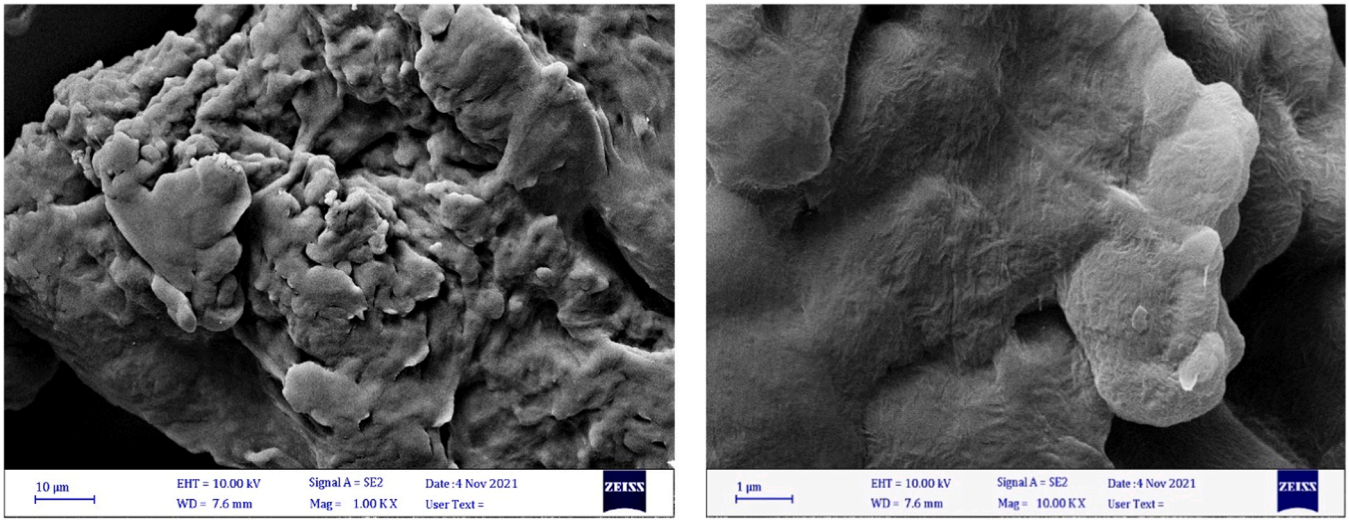

Fig. 2. SEM images of microplastic adsorbent.

provides an estimation of the pore volume and surface area. The nitrogen adsorption-desorption isotherm of microplastic is represented in Fig. 4. Based on the IUPAC categorization, microplastic isotherm is categorized as type II with hysteresis, which indicates the non-porous and macroporous nature of the adsorbent. Also, the BET-specific surface area and mean pore size of microplastic particles are tabulated in Table 2.

3.2. Evaluation of effective adsorption parameters

3.2.1. pH influence

The results of the pH effect on the MB removal by the microplastic adsorbent in Fig. 5 show that with an increase in pH from 2 to 7, there was a corresponding increase in adsorption. However, there was a decrease in adsorption from pH 7–8, followed by another rise at pH 10. Based on the data, the optimal pH for MB removal using the microplastic adsorbent was 7, with an adsorption capacity of 3.9 mg/g and a removal efficiency of 65%. The pH of the solution can impact the speciation of MB in the solution and the surface charge distribution on MB. As a result, the electrostatic interactions between the different species of MB in the solution and the surface of the microplastic can be affected, leading to attractive or repulsive forces. MB appears under the influence of the aqueous solution pH in two cationic species and undissociated molecules (Fig. 6). At pH 3, the MB species prevails, accounting for 86% of the total species. At the pH equal to the pK_a value of 3.8, both MB° and MB^{+} species coexist in equal proportions of 50%. However, at pH greater than 6, the MB^{+} species becomes nearly the exclusive form of MB present [59]. According to studies conducted by Xu et al. [47] and You et al. [34], the zero charge point (pH_{pzc}) of polyethylene is 4.3, which means that the surface charge of the polyethylene microplastic is positively charged when the pH is lower than 4.3. The reason for the low adsorption capacity of the microplastic adsorbent at pH values lower than pH_{pzc} is attributed to the electrostatic repulsion between the positively charged surface of the microplastic adsorbent and electro-positive MB (cationic) in the aqueous solution. Besides, the excess H^{+} ions in the solution compete with the MB^{+} ions for adsorption

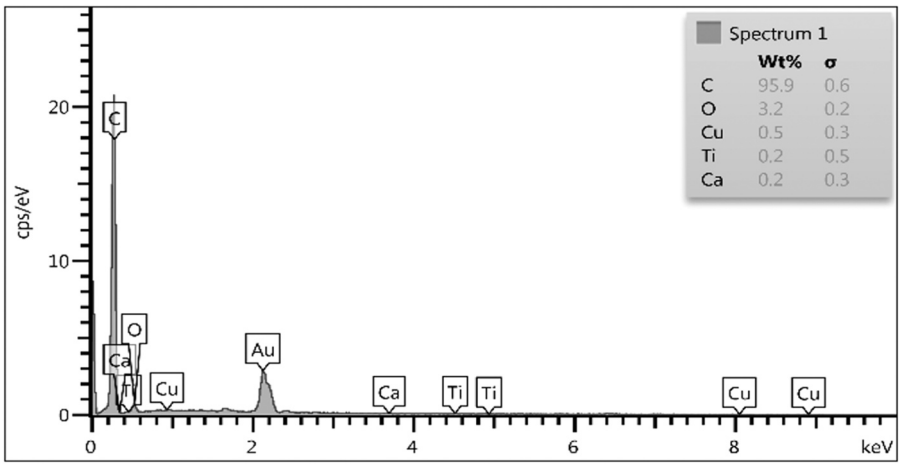

Fig. 3. EDS spectrum of microplastic.

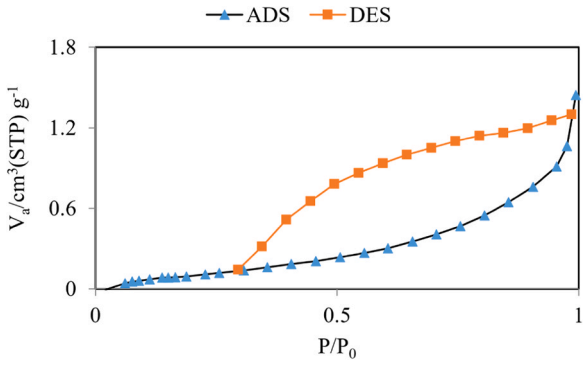

Fig. 4. Nitrogen adsorption-desorption isotherms of microplastic adsorbent.

Table 2
Results of BET analysis performed on microplastic.

Parameter	Value
Specific surface area (m^2/g)	0.6865
Average volume of cavities (cm^3/g)	0.002
Average hole diameter (nm)	12.228

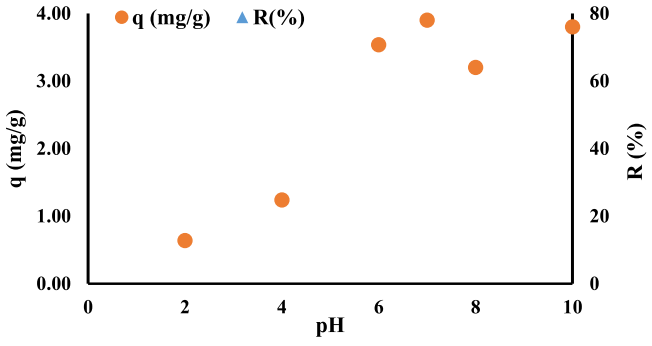

Fig. 5. The impact of pH on the removal efficiency and the adsorption capacity of MB by the microplastic adsorbent (initial concentration 20 mg/L, adsorbent dose 0.1 g, time 30 min, and temperature 25 °C).

sites on the microplastic adsorbent, leading to a decrease in adsorption under acidic conditions. The interaction between the hydroxyl groups on the surface of the polyethylene microplastics and the nitrogen atoms of MB leads to the formation of hydrogen bonding, which is the primary

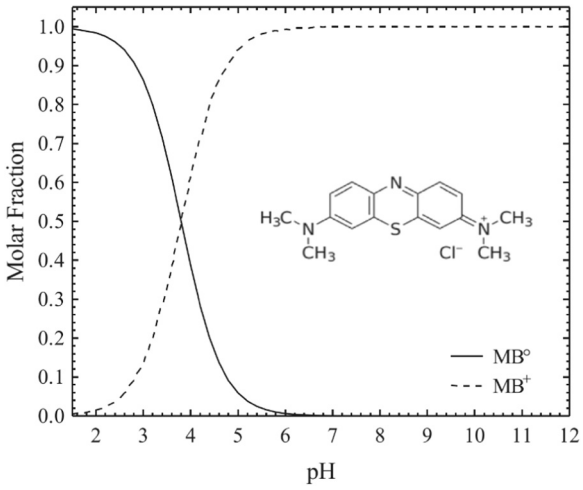

Fig. 6. Molecular structure and speciation diagram of the MB [59].

adsorption mechanism at low pH values. With increasing pH, the surface charge of the microplastic adsorbent becomes negative at pH> 4.3. In contrast, the dominant species of MB at pH> 3.8 is cationic, which leads to an enhancement in the electrostatic attraction between them, and the adsorption capacity increases.

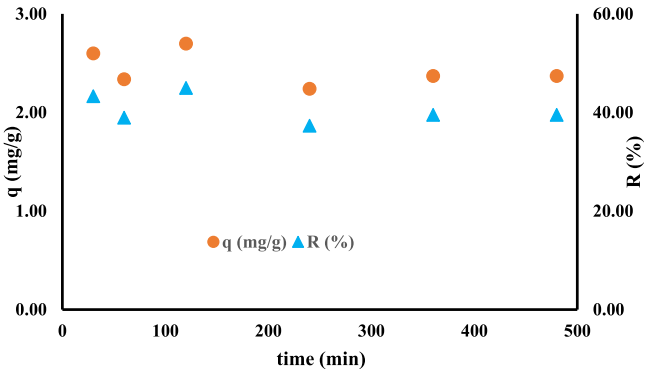

Fig. 7. The contact time influence on the removal efficiency and the adsorption capacity of MB by the microplastic adsorbent (initial concentration 20 mg/L, adsorbent dose 0.1 g, pH 7, and temperature 25 °C).

3.2.2. Contact time influence

The results of the contact time influence on the MB dye elimination by microplastics are shown in Fig. 7. The highest removal of the pollutant occurred in the first minutes, which can be ascribed to the empty sorption sites at the beginning of the adsorption process [50,51]. The optimal contact time for adsorption was determined to be 30 min, based on the results that showed a removal efficiency of 43.32% and an adsorption capacity of 2.60 mg/g. According to the findings of You et al. [34], the amount of MB adsorbed onto the aged polyethylene microplastics increased progressively over time and eventually reached equilibrium after 72 hours.

3.2.3. Initial concentration influence

According to the findings illustrated in Fig. 8, when the initial concentration of MB was increased from 1 to 10 mg/L, the removal efficiency decreased. However, it reached a maximum value of 72.35% when the initial concentration was 20 mg/L. On the other hand, the adsorption capacity increased with the enhancement in the initial concentration of cationic dye. The observed phenomenon can be diagnosed as follows: at lower pollutant concentration levels, there are more available adsorption sites on the adsorbent surface. As more pollutants adsorb onto the surface, available sites become saturated faster, decreasing removal efficiency for MB pollutants [8,60]. The increase in adsorption capacity observed with the increasing initial concentration of MB may be due to the probable interaction between the MB ions and the surface of the adsorbent. Hameed et al. [60] stated that a higher initial dye concentration results in a higher adsorption capacity due to a more significant concentration gradient, which creates a more vital driving force for mass transfer. Similar results have been reported by Arshadi et al. [8], Amiri et al. [9], and Bahrami et al. [16].

3.2.4. Adsorbent dosage influence

Fig. 9 indicates the results of the adsorbent dosage effect on MB removal efficiency and MP adsorption capacity. Enhancement in the sorbent dosage from 0.1 to 1 g raised the removal efficiency of MB pollutants from 52.29% to 75.23% because of the increment in the surface area and the number of available adsorption sites [50]. Contrariwise, as the adsorbent dose increased, the adsorption capacity decreased due to a reduction in the amount of MB adsorbed per unit weight of the adsorbent [44,51,61]. Furthermore, an increase in the dosage of the MP creates a more pronounced concentration gradient between the MB solution and the surface of the MP. This concentration gradient facilitates the movement of MB molecules from the bulk solution toward the MP surface, thereby enhancing the chances of adsorption occurrence [44].

3.2.5. Temperature influence

The graph depicted in Fig. 10 illustrates that the maximum removal efficiency of MB was achieved at a temperature of 40 °C, with a value of 52.03%. The decrease in adsorption as the temperature of the MB solution increased from 40 to 60 °C suggests a weak adsorption interaction of MB on the adsorbent surface [43]. The reduction in MB adsorption in the temperature range of 40–60 °C can be attributed to several factors, including thermodynamic effects, solubility and diffusion, and changes in microplastic structure [43]. The findings indicate that the adsorption of MB by the microplastic adsorbent is an exothermic process [62]. At elevated temperatures, the boundary layer thickness reduces because MB has a greater tendency to desorb from the adsorbent surface and return to the solution phase, and subsequently, the adsorption decreases. Elevated temperatures can increase the solubility of MB, allowing more dye molecules to remain in the liquid phase instead of adsorbing onto microplastic surfaces. Furthermore, elevated temperatures can accelerate the diffusion rate of MB molecules, enabling them to traverse the solution more swiftly. This heightened diffusion rate restricts their interaction with the microplastic surface, which limits adsorption. Rising temperatures can cause alterations in the properties and structure of polyethylene microplastics. These changes may involve the softening or melting of the microplastic material, resulting in altered surface characteristics and diminished adsorption capacity.

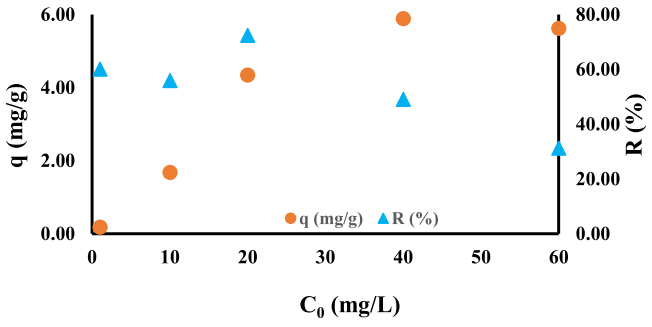

Fig. 8. The initial concentration influence on the removal efficiency and the adsorption capacity of MB by the microplastic adsorbent (initial concentrations 1–60 mg/L, adsorbent dose 0.1 g, time 30 min, pH 7, and temperature 25 °C).

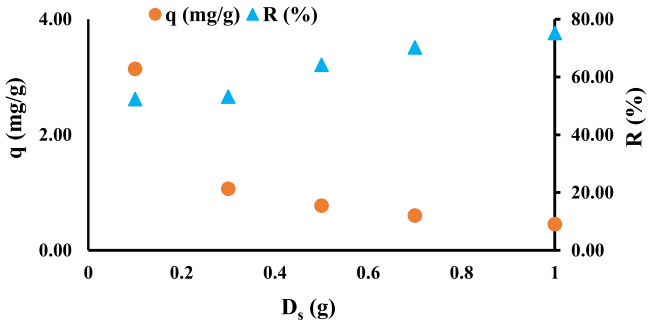

Fig. 9. The adsorbent dosage influence on the removal efficiency and the adsorption capacity of MB by the microplastic adsorbent (initial concentration 20 mg/L, contact time 30 min, pH 7, and temperature 25 °C).

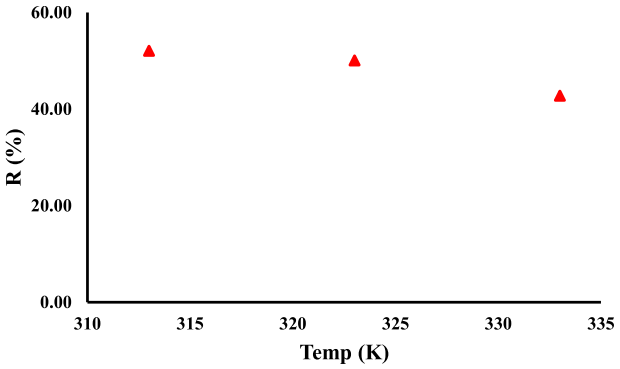

Fig. 10. The influence of temperature on the removal efficiency and the adsorption capacity of MB by the microplastic adsorbent (initial concentration 20 mg/L, adsorbent dose 0.1 g, time 30 min, and pH 7).

3.3. Adsorption kinetics

Based on the outcomes of the batch adsorption tests, the adsorption rates were explored by kinetic studies. Table 3 presents the kinetic models' variables calculated via non-linear regression. Based on the coefficient of determination and Friedman's average rank method, the F-P model was the most appropriate kinetic model for characterizing MB removal. Next, the PSO model was fitted on experimental data, and the calculated value of q_e (2.627 mg/g) was in close agreement with the experimental q_e value of 2.60 mg/g. That is, the multiple interfacial interactions, such as hydrophobic partitioning, electrostatic attraction,

Table 3
The kinetic parameters and error functions obtained for MB dye adsorption by microplastic.

Model	PFO	PSO	Elovich	F-P
$q_{e,exp}$ = 2.60				
Coefficients	q_e=2.53 k=0.05	q_e=2.627 k=0.05	α=50 β=4.301	a=2.861 b=-0.032
R^2	0.9840	0.9863	0.9808	0.9968
RMSE	0.31	0.28	0.34	0.14
SSE	0.57	0.48	0.68	0.11
SAE	0.57	0.48	0.68	0.11
ARE	1.50	1.31	1.82	0.31
HYBRID	1.001	9.89	12.68	4.30
MPSD	12.26	11.47	13.51	5.61
Average rating of Friedman	2.71	2.14	4	1.14
Model rating	3	2	4	1

hydrogen bonding, and van der Waals forces, were closely related to the rate-determining step [63] (Zhang et al., 2020). These results are expressive of the chemisorption of MB by MP adsorbent.

The constant values of the Elovich model (α and β) for MB adsorption on the microplastic particles express the effect of the adsorbent dose and the possibility of carrying out adsorption and desorption cycles. Based on the findings of the studies of Awwad et al. [64] and Basu et al. [61], these parameters provide an acceptable value in removing MB dye from the aqueous solution. Friedman's rank indicated that despite the potential impact of the Elovich model constants, the model did not fit well with the experimental data.

3.4. Adsorption isotherm

Table 4 displays the constants for the isotherm models, which were determined through non-linear regression. These constants can be used to predict adsorption capacities and to incorporate them into mass transfer relationships to design adsorption experiments. The high R^2 and low error values demonstrate the suitability of the R-P model for MB adsorption onto MP materials. The successful fitting of the adsorption data to the Redlich-Peterson model indicates that the removal of MB occurs through multilayer adsorption on the heterogeneous surface of the MP adsorbent [65]. SEM observations are also consistent with these results. Lin et al. [66] stated that the Redlich-Peterson method results from combining the Langmuir and Freundlich isotherm equations, which is suitable for porous adsorbents. Based on the average rating of Friedman, the Temkin isotherm is ranked second. The high value of the b_T constant, the relationship between the logarithm of the equilibrium concentration and the adsorption rate, indicates that the adsorption has been done well. The Langmuir model, which has a Friedman rank of three, cannot describe the nature of the adsorption process well. As the assumptions of this model are based on the uniform surface of the adsorbent, each adsorption site can adsorb only one species. These assumptions are inconsistent with the results and do not conform to SEM analysis [67]. As shown in Fig. 11, the dimensionless separation factor (R_L) values obtained from the Langmuir model are less than 1 ($0.0001 < R_L < 0.011$), indicating that the adsorption process is favorable [48]. The last simulation model is the Freundlich isotherm model, utilized to describe the adsorption on heterogeneous surfaces and accounts for the development of multilayer adsorption and interactions between adsorbing molecules [68]. As can be seen, the adsorption desirability index (n) in the Freundlich model for microplastic adsorbent was more than 1, which indicates a favorable physical process.

Table 4
Non-linear isotherm parameters and error functions acquired for the adsorption of MB dye by microplastics.

Model	Langmuir	Freundlich	R-P	Temkin
Coefficients	b = 87.127 q_m =1.205	K_F = 1.099 n = 20	a = 2.0 b=18	A_T = 1.0 b_T = 157.65
R^2	0.9995	0.9777	0.9527	0.6334
RMSE	0.9871	0.9764	0.9650	0.8003
SSE	4.87	4.76	4.65	3.20
SAE	4.87	4.76	4.65	3.20
ARE	89.54	87.98	10.03	28.71
HYBRID	79.422	79.427	19.700	52.360
MPSD	94.63	93.79	31.67	53.58
Average rating of Friedman	3.42	1.57	1.71	1.85
Model rating	3	4	1	2

3.5. Adsorption thermodynamics

To gain a better understanding of how increasing temperature impacts the adsorption of MB dye onto MP particles, three fundamental thermodynamic parameters were examined: the Gibbs free energy of adsorption (ΔG), the enthalpy change (ΔH), and the entropy change (ΔS). The obtained values of thermodynamic factors are presented in Fig. 12. The fact that the Gibbs free energy values are negative indicates that the adsorption of MB on the microplastic material is thermodynamically favorable and is carried out through a spontaneous process. On the other hand, the ΔG value increased as the temperature increased, suggesting better adsorption occurs at lower temperatures [68]. The negative magnitude of ΔH (-25.05 kJ/mol) confirms that the adsorption process is exothermic, consistent with the observed decrease in MB uptake by the MP as the temperature increases. Also, based on the magnitude of ΔH, it appears that the MB dye adsorption by the microplastic adsorbent is a chemical process characterized by strong interactions between the MB particles and the functional groups on the MP surface. According to Ozdes et al. [68] and Khormaei et al. [69], the enthalpy value provides information about the adsorption type. Typically, the ΔH value for physical adsorption is less than 4.2 kJ/mol, while it is greater than 21 kJ/mol for chemical adsorption. The negative magnitude of ΔS (-0.03048 kJ/mol) proposed a declined randomness at the solid/solution interface during the adsorption of MB dye on the MP surface. A similar trend was observed by Khormaei et al. [69], who demonstrated that an increase in temperature from 20 to 50 °C resulted in a decrease of approximately 20% in copper removal.

The outcome suggests that the impact of MP on the coexisting species in its vicinity may vary depending on the season and location. MP adsorption may be more severe in winter and colder regions, but negligible in summer and hotter areas.

3.6. Desorption

As can be seen in the results of the adsorption-desorption processes in five cycles in Fig. 13, the reusability of the adsorbent exhibits promising outcomes. Because microplastic could remove MB dye up to five cycles, and the change in adsorbability was not so much. Therefore, the microplastic can act as a cost-effective and practical adsorbent for removing MB pollutants from an aqueous environment. The findings

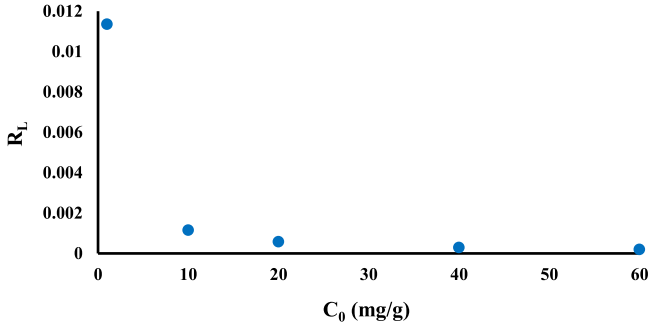

Fig. 11. The separation factor of the Langmuir model for various values of initial concentration.

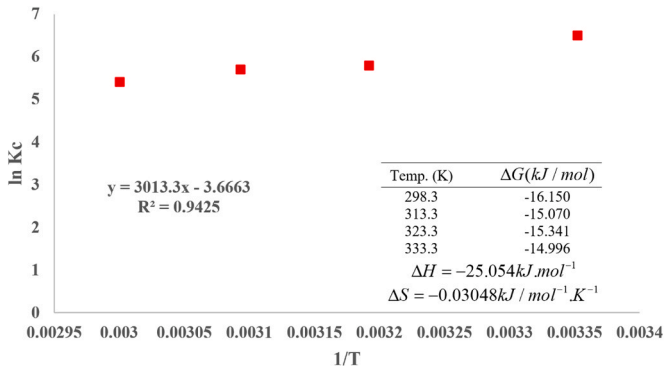

Fig. 12. The van't Hoff graph of ln (K_C) vs. 1/T for MB uptake by microplastics.

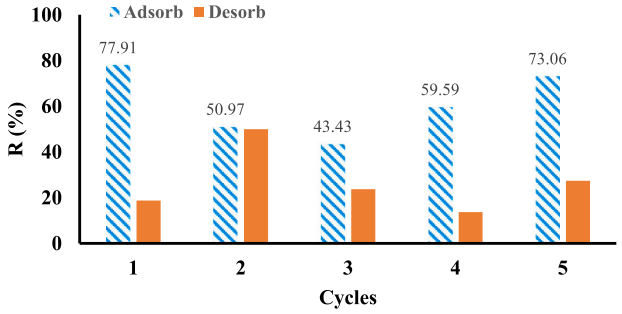

Fig. 13. Adsorption- desorption cycles of MB dye by the microplastic adsorbent.

were consistent with the research performed by Tsade Kara et al. [70] in the reuse of modified nano cellulose adsorbent to eliminate MB dye. According to You et al. [34], the desorption efficiency of adsorbed MB can significantly vary depending on the physiological conditions of the organisms in question. They also proposed that the MB adsorbed onto MP could potentially be desorbed following ingestion by marine organisms.

3.7. Mechanism studies

It has been observed that materials with a negatively charged surface tend to attract cationic species through electrostatic attraction. However, the amount of adsorbed cationic species is not always higher than that of anionic species, suggesting that other complex interactions may also be involved in adsorption [71]. It is worth noting that, according to the value of logKow (5.85) of MB and the contact angle (CA) of MP, the hydrophobicity of the surface of MP and MB molecules is stronger with a larger logKow or CA value [72]. Therefore, hydrophobic partitioning plays an essential role in the sorption of MB onto the MP. Additionally, the electrostatic attraction between the cationic MB and the negative charges on MP and hydrogen bonding also contribute to the capture of MB.

3.8. Random forest regression modeling

Two indices, namely %IncMSE and IncNodePurity, were utilized to determine the relative importance of various parameters and optimize the adsorption process. The %IncMSE index measures the increase in mean squared error when a particular parameter is randomly permuted. A higher %IncMSE value indicates that the permutation of that parameter has a more significant impact on the adsorption capacity. By analyzing the %IncMSE values for each parameter, it becomes possible to identify the most influential factors. The IncNodePurity index evaluates the enhancement in node purity when a decision tree is split based on a specific parameter. A higher IncNodePurity value indicates a greater contribution of the parameter to the overall predictability of the model. By scrutinizing the IncNodePurity values, one can ascertain the relative importance of each parameter in predicting the adsorption capacity. Random forest regression (RFR) was employed to simulate the non-linear behavior of the adsorption process. The results, depicted in Fig. 14 and Table 5, illustrate the modeled adsorption capacity (q) of MP for the removal of MB from aqueous solution under the effect of various independent variables, including pH, temperature, reaction time, adsorbent dosage, and initial concentration of MB.

The outputs obtained from Random Forest Regression reveal that the adsorption capacity of the MP is primarily influenced by the adsorbent dose (C_s), followed by C_0, pH, time, and temperature. This conclusion is drawn based on the percent increase in mean squared error (%IncMSE index) as an indicator of variable importance. Additionally, when considering the increase in node purity (IncNodePurity index), the parameters were ranked in the following order of importance for the adsorption capacity of MP: C_0, C_s, pH, time, and temperature. Based on the average rank values of both indices presented in Table 6, C_0 and dose (C_s) have the highest impact on the adsorption capacity (q). On the other hand, pH, time, and temperature have comparatively lower rankings, indicating a relatively lesser influence on the adsorption capacity. Therefore, according to the RFR technique, the variables C_0 and C_s were identified as the most influential predictors of the adsorption capacity. Fig. 15 confirms this result and reveals that two parameters significantly affect the adsorption capacity. The coefficient of determination (R^2) for the model's predictability was 97.55%, which indicates a high degree of accuracy and reliability of the random forest regression model. To obtain a comprehensive understanding of how each parameter collectively influences the adsorption capacity of MP, we considered the combined impact of all factors. According to Fig. 16, it can be observed that there is a positive correlation between the pH and the adsorption capacity of MP. As the pH increases, the adsorption capacity of MP also increases. Notably, there is a steep increase in the adsorption capacity at pH levels around 4–5, and this upward trend continues up to around pH 10. Since dye precipitation occurs in alkaline pHs, the optimal pH value for maximum adsorption capacity equals 7.

Adsorption capacity reduction with time is divided into two stages: at first, MB is quickly adsorbed on the microplastics within 30 min, and then q is decreased sharply up to 120 min. After that, the adsorption capacity reduced less intensively with time [44]. An enhancement in the initial concentration of MB caused a growth in the adsorption capacity of microplastics. One explanation for this phenomenon is that a higher dye initial concentration creates a more potent driving force for mass transfer, resulting in a higher adsorption capacity [60]. By increasing the adsorbent dose, the adsorption capacity of MP declined because of the accumulation of adsorbent particles in the solution, which creates diffusion and migration barricades that prevent pollutant molecules from reaching the adsorbent surface [61,73]. The adsorption capacity of MP was found to decrease as the temperature increased, with the highest value of q being observed at a temperature below 40 °C. In contrast, the q falling slope at 50–60 °C is greater than that of 40–50 °C.

4. Conclusion

This study employs a random forest regression model to predict the batch adsorption of MB onto polyethylene microplastics. This modeling approach provides a novel and potentially more accurate method for understanding and predicting the adsorption behavior compared to traditional linear models typically used in similar studies. The adsorption process considered various factors, including pH (2−10), initial concentration of MB (1–60 mg/L), contact time (30–480 min), temperature (40–60 °C), and adsorbent dose (0.1–1 g). Batch adsorption studies revealed that the optimum removal of MB was achieved at a pH level of 7. Additionally, it was observed that equilibrium between the adsorbent and MB was attained after a contact time of 30 min. The results from the

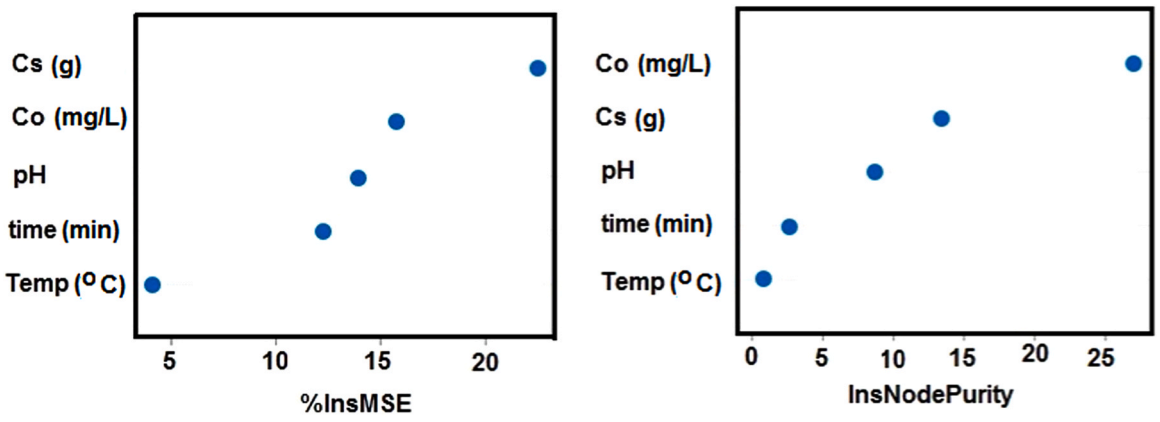

Fig. 14. Variable significance estimated by RFR.

Table 5
Variable significance estimated by RFR.

parameter	%IncMSE	IncNodePurity
pH	13.93	8.59
time	12.35	2.67
C_0	15.70	27.17
C_s	22.48	13.43
Temp	4.15	0.88

Table 6
The rank of parameters' significance on q based on RFR.

Parameter	I_1	I_2	Mean rank
C_0	2	1	1.5
C_s	1	2	1.5
pH	3	3	3
time	4	4	4
Temp	5	5	5

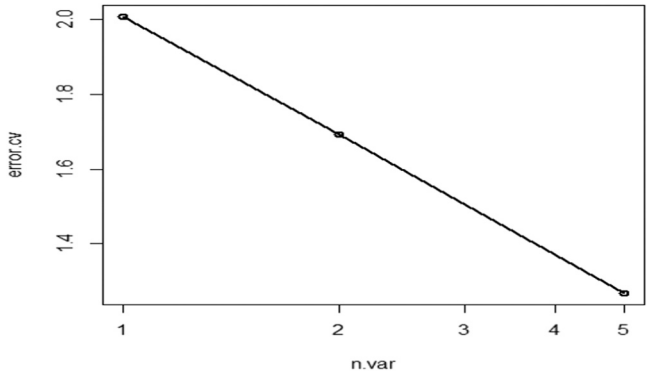

Fig. 15. Number of the most influential variables in predicting q.

kinetic and isotherm studies suggest that the adsorption of MB follows a chemisorption mechanism during the multilayer adsorption process on the heterogeneous surface of the MP adsorbent. The thermodynamic evaluation indicated that the adsorption of MB was a spontaneous and exothermic process, with the highest removal of MB occurring at 40 °C. The adsorption process was found to occur through both chemical and physical mechanisms. The reusability of MP was corroborated with promising results after five cycles of adsorption-desorption of MB dye. SEM characterization analysis showed the non-porous microplastic structure owning holes, in which the shape of the holes is irregular and chaotic. BET study indicated the non-porous and macroporous nature of the MP adsorbent. Also, FTIR minor changes in the molecular structure before and after the adsorption tests illustrated that the microplastic adsorbent was successful in adsorbing MB. The random forest regression was able to model the adsorption process satisfactorily. The sensitivity analysis of the model revealed that the adsorption of MB onto the microplastic adsorbent is more sensitive to changes in the initial MB concentration and the amount of adsorbent used. This modeling approach can be valuable in practical applications by providing insights into the factors influencing the adsorption process and facilitating optimization efforts. The combination of experimental and modeling approaches enhances our understanding of the potential use of polyethylene microplastics in water treatment and provides a foundation for further research in this area.

Ethical approval

This manuscript does not contain any study with humans and animals performed by any of the authors.

Funding information

The authors declare that no funds, grants, or other support were received during the preparation of this manuscript.

Author contributions

M. Bahrami and M.J. Amiri conceived and designed the experiments; S. Rajabi carried out the experiments; M. Bahrami and M.R. Mahmoudi analyzed the data; M. Bahrami and S. Rajabi wrote the paper with aid of M.J. Amiri. All authors have read and agreed to the published version of the manuscript

Consent to participate

is not applicable.

Consent for publication

The authors have consented to the submission of the study to the journal.

Declaration of Competing Interest

The authors have no relevant financial or non-financial interests to disclose.

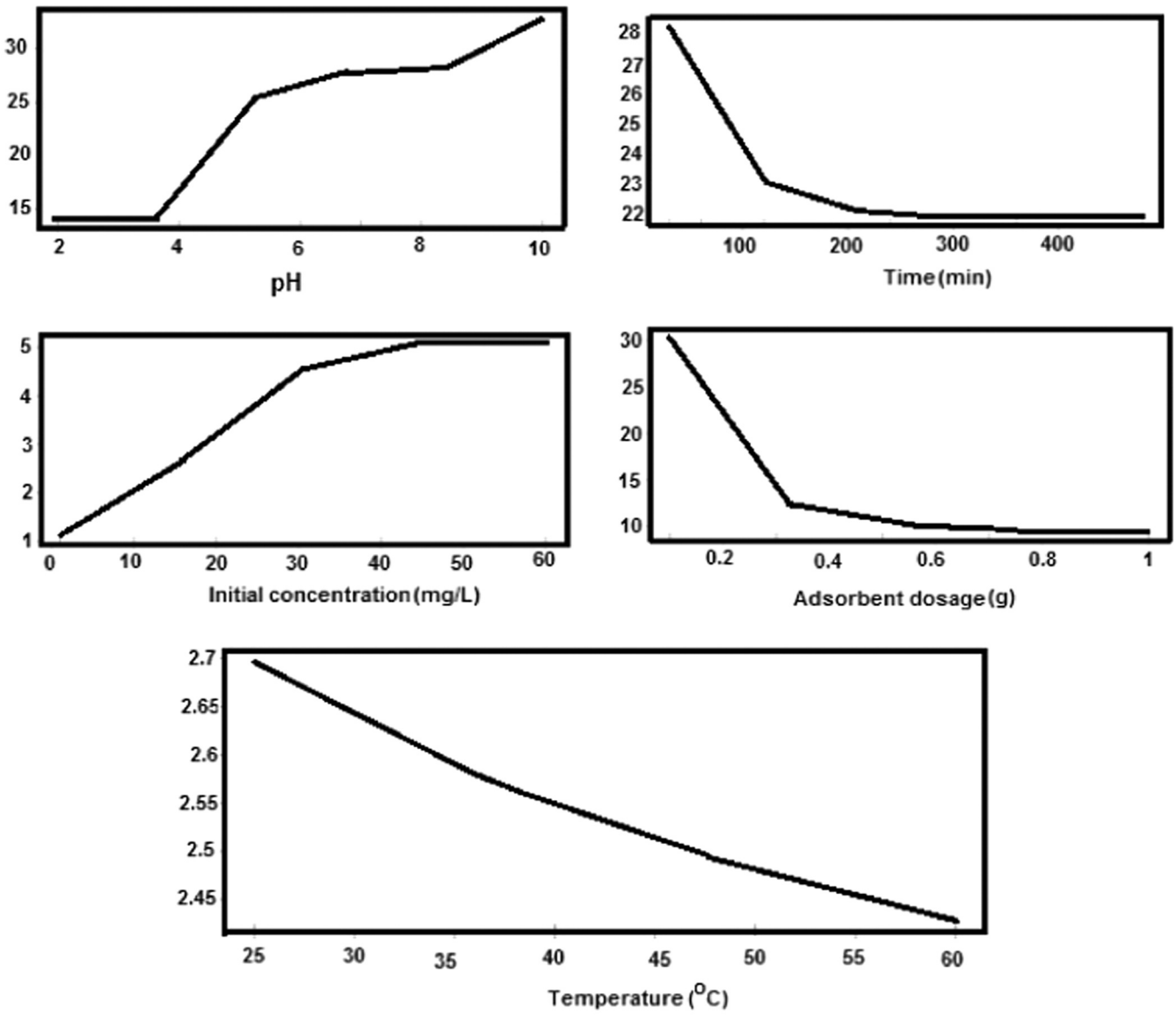

Fig. 16. Performing sensitivity analysis on the effective parameters of adsorption capacity using RFR.

Data Availability

Due to ethical reasons data were not provided in the manuscript but will be available on request.

Acknowledgement

This study was conducted as part of a master's thesis. The authors would like to express their gratitude to Fasa University for their partnership and support.

References

[1] X. Jin, M. Nodehi, M. Baghayeri, Y. Xu, Z. Hua, Y. Lei, M. Shao, P. Makvandi, Development of an impedimetric sensor for susceptible detection of melatonin at picomolar concentrations in diverse pharmaceutical and human specimens, Environ. Res. 238 (2023) 117080, https://doi.org/10.1016/j.envres.2023.117080.

[2] X. Jin, M. Baghayeri, M. Nodehi, M.-S. Koshki, A. Ramezani, M. Fayazi, Y. Xu, Z. Hua, Y. Lei, P. Makvandi, Evaluation of thallium ion as an effective ion in human health using an electrochemical sensor, Environ. Res. 238 (2023) 117026, https://doi.org/10.1016/j.envres.2023.117026.

[3] J. You, J. Li, Z. Wang, M. Baghayeri, H. Zhang, Application of Co_3O_4 nanocrystal/rGO for simultaneous electrochemical detection of cadmium and lead in environmental waters, Chemosphere 335 (2023) 139133, https://doi.org/10.1016/j.chemosphere.2023.139133.

[4] L. Baloo, M.H. Isa, N.Bin Sapari, A.H. Jagaba, L.J. Wei, S. Yavari, R. RazaliL, R. Vasuet, Adsorptive removal of methylene blue and acid orange 10 dyes from aqueous solutions using oil palm wastes-derived activated carbons, Alex. Eng. J. 60 (6) (2021) 5611–5629, https://doi.org/10.1016/j.aej.2021.04.044.

[5] S. Eslamian, Urban Water Reuse Handbook, CRC Press, Boca Raton, FL, USA, 2015, p. 1177, https://doi.org/10.1201/b19646.

[6] T. Feng, F. Zhang, J. Wang, L. Wang, Application of chitosan-coated quartz sand for congo red adsorption from aqueous solution, J. Appl. Polym. Sci. 125 (3) (2012) 1766–1772, https://doi.org/10.1002/app.35670.

[7] S. Madduri, I. Elsayed, E.B. Hassan, Novel oxone treated hydrochar for the removal of Pb (II) and methylene blue (MB) dye from aqueous solutions, Chemosphere 260 (2020) 127683, https://doi.org/10.1016/j.chemosphere.2020.127683.

[8] M. Arshadi, M. Mehravar, M.J. Amiri, A.R. Faraji, Synthesis and adsorption characteristics of an heterogenized manganese nanoadsorbent towards methyl orange, J. Colloid Interface Sci. 440 (2015) 189–197, https://doi.org/10.1016/j.jcis.2014.10.053.

[9] M.J. Amiri, M. Raayatpisheh, M. Radi, S. Amiri, Preparation and characterization of biopolymer-based adsorbents and their application for methylene blue removal from wastewater, Sci. Rep. 13 (1), 17263, https://doi.org/10.1038/s41598-023-44613-6.

[10] M.J. Amiri, A. Faraji, M. Azizi, B. Goudarzi Nejad, M. Arshadi, Recycling bone waste and cobalt-wastewater into a highly stable and efficient activator of peroxymonosulfate for dye and HEPES degradation, Process Saf. Environ. Prot. 147 (2021) 626–641, https://doi.org/10.1016/j.psep.2020.12.039.

[11] Y.A. Bustos-Terrones, J.J. Hermosillo-Nevárez, B. Ramírez-Pereda, M. Vaca, J. G. Rangel-Peraza, V. Bustos-Terrones, M.N. Rojas-Valencia, Removal of BB9 textile

dye by biological, physical, chemical, and electrochemical treatments, J. Taiwan Inst. Chem. Eng. 121 (2021) 29–37, https://doi.org/10.1016/j.jtice.2021.03.041.
[12] L. Huang, Q. Shuai, S. Hu, Tannin-based magnetic porous organic polymers as robust scavengers for methylene blue and lead ions, J. Clean. Prod. 215 (2019) 280–289, https://doi.org/10.1016/j.jclepro.2019.01.040.
[13] H. Koyuncu, A.R. Kul, Removal of methylene blue dye from aqueous solution by nonliving lichen (Pseudevernia furfuracea (L.) Zopf.), as a novel biosorbent, Appl. Water Sci. 10 (2020) 72, https://doi.org/10.1007/s13201-020-1156-9.
[14] F.M. Mpatani, A.A. Aryee, A.N. Kani, K. Wen, E. Dovi, L. Qu, Z. Li, R. Han, Removal of methylene blue from aqueous medium by citrate modified bagasse: kinetic, equilibrium and thermodynamic study, Bioresour. Technol. Rep. 11 (2020) 100463, https://doi.org/10.1016/j.biteb.2020.100463.
[15] M.J. Amiri, M. Bahrami, M. Badkouby, I.K. Kalavrouziotis, Greywater Treatment Using Single and Combined Adsorbents for Landscape Irrigation, Environ. Process. 6 (1) (2019) 43–63, https://doi.org/10.1007/s40710-019-00362-1.
[16] M. Bahrami, M.J. Amiri, F. Bagheri, Optimization of the lead removal from aqueous solution using two starch based adsorbents: design of experiments using response surface methodology (RSM), J. Environ. Chem. Eng. 7 (1) (2019) 102793, https://doi.org/10.1016/j.jece.2018.11.038.
[17] M. Akin, R. Bayat, M. Bekmezci, Z.K. Coguplugil, F. Sen, M. Baghayeri, A. Kaffash, F. Tehranejad-Javazmi, I. Sheikhshoaie, The use of polymer/carbon based material as an efficient and low-cost electrochemical sensor for rapid electrochemical detection of dopamine, Carbon Lett. (2023), https://doi.org/10.1007/s42823-023-00537-9.
[18] A. Amiri, M. Baghayeri, M. Shahabizadeh, Polypyrrole/carbon nanotube coated stainless steel mesh as a novel sorbent, N. J. Chem. 47 (2023) 4402–4408, https://doi.org/10.1039/D2NJ04837J.
[19] W. Sun, Y. Hong, T. Li, H. Chu, J. Liu, L. Feng, M. Baghayeri, Biogenic synthesis of reduced graphene oxide decorated with silver nanoparticles (rGO/Ag NPs) using table olive (Olea europaea) for efficient and rapid catalytic reduction of organic pollutants, Chemosphere 310 (2023) 136759, https://doi.org/10.1016/j.chemosphere.2022.136759.
[20] M. Bahrami, M.J. Amiri, F. Bagheri, Optimization of crystal violet adsorption by chemically modified potato starch using response surface methodology, Pollution 6 (2020) 159–170, https://doi.org/10.22059/poll.2019.288467.674.
[21] D.K. Kanhai, K. Gardfeldt, O. Lyashevska, M. Hassellov, R.C. Thompson, I. O'Connor, Microplastics in sub-surface waters of the Arctic Central Basin, Mar. Pollut. Bull. 130 (2018) 8–18, https://doi.org/10.1016/j.marpolbul.2018.03.011.
[22] A.A. Franco, J.M. Arellano, G. Albendín, R. Rodríguez-Barroso, J.M. Quiroga, M. D. Coello, Microplastic pollution in wastewater treatment plants in the city of Cádiz: abundance, removal efficiency and presence in receiving water body, Sci. Total Environ. 776 (2021) 145795, https://doi.org/10.1016/j.scitotenv.2021.145795.
[23] S. Acarer, Microplastics in wastewater treatment plants: sources, properties, removal efficiency, removal mechanisms, and interactions with pollutants, Water Sci. Technol. 87 (2023) 685–710, https://doi.org/10.2166/wst.2023.022.
[24] M.R. Karimi Estahbanati, M. Kiendrebeogo, A. Khosravanipour Mostafazadeh, P. Drogui, R.D. Tyagi, Treatment processes for microplastics and nanoplastics in waters: state-of-the-art review, Mar. Pollut. Bull. 168 (2021) 112374, https://doi.org/10.1016/j.marpolbul.2021.112374.
[25] H.J. Kwon, H. Hidayaturrahman, S.G. Peera, T.G. Lee, Elimination of microplastics at different stages in wastewater treatment plants, Water 14 (15) (2022) 2404, https://doi.org/10.3390/w14152404.
[26] M. Nikpay, Wastewater fines influence the adsorption behavior of pollutants onto microplastics, J. Polym. Environ. 30 (2022) 776–783, https://doi.org/10.1007/s10924-021-02243-x.
[27] A. Puckowski, W. Cwięk, K. Mioduszewska, P. Stepnowski, A. Białk-Bielińska, Sorption of pharmaceuticals on the surface of microplastics, Chemosphere 263 (2021) 127976, https://doi.org/10.1016/j.chemosphere.2020.127976.
[28] J. Yao, J. Wen, H. Li, Y. Yang, Surface functional groups determine adsorption of pharmaceuticals and personal care products on polypropylene microplastics, J. Hazard. Mater. 423 (2022) 127131, https://doi.org/10.1016/j.jhazmat.2021.127131.
[29] Q. Mo, X. Yang, J. Wang, H. Xu, W. Li, Q. Fan, S. Gao, W. Yang, C. Gao, D. Liao, Y. Li, Y. Zhang, Adsorption mechanism of two pesticides on polyethylene and polypropylene microplastics: DFT calculations and particle size effects, Environ. Pollut. 291 (2021) 118120, https://doi.org/10.1016/j.envpol.2021.118120.
[30] Y. Dong, M. Gao, Z. Song, W. Qiu, Adsorption mechanism of As(III) on polytetrafluoroethylene particles of different size, Environ. Pollut. 254 (2019) 112950, https://doi.org/10.1016/j.envpol.2019.07.118.
[31] X. Guo, G. Hu, X. Fan, H. Jia, Sorption properties of cadmium on microplastics: the common practice experiment and a two-dimensional correlation spectroscopic study, Ecotoxicol. Environ. Saf. 190 (2020) 110118, https://doi.org/10.1016/j.ecoenv.2019.110118.
[32] S. Tang, L. Lin, X. Wang, A. Feng, A. Yu, Pb(II) uptake onto nylon microplastics: interaction mechanism and adsorption performance, J. Hazard Mater. 386 (2020) 121960, https://doi.org/10.1016/j.jhazmat.2019.121960.
[33] L. Lin, S. Tang, X.S. Wang, X. Sun, Z. Han, Y. Chen, Accumulation mechanism of tetracycline hydrochloride from aqueous solutions by nylon microplastics, Environ. Technol. Innov. 18 (2020) 100750, https://doi.org/10.1016/j.eti.2020.100750.
[34] H. You, B. Huang, C. Cao, X. Liu, X. Sun, L. Xiao, et al., Adsorption–desorption behavior of methylene blue onto aged polyethylene microplastics in aqueous environments, Mar. Pollut. Bull. 167 (2021) 112287, https://doi.org/10.1016/j.marpolbul.2021.112287.
[35] M. Zhao, L. Huang, S.R.B. Arulmani, J. Yan, L. Wu, L. Wu, T. Zhang, H. Xiao, Adsorption of different pollutants by using microplastic with different influencing factors and mechanisms in wastewater: a review (T.), Nanomater 12 (2022) 2256, https://doi.org/10.3390/nano12132256.
[36] L. McDougall, L. Thomson, S. Brand, A. Wagstaff, L.A. Lawton, B. Petrie, Adsorption of a diverse range of pharmaceuticals to polyethylene microplastics in wastewater and their desorption in environmental matrices, Sci. Total Environ. 808 (2022) 152071, https://doi.org/10.1016/j.scitotenv.2021.152071.
[37] B. Gui, X. Xu, S. Zhang, Y. Wang, C. Li, D. Zhang, L. Su, Y. Zhao, Prediction of organic compounds adsorbed by polyethylene and chlorinated polyethylene microplastics in freshwater using QSAR, Environ. Res. 197 (2021), https://doi.org/10.1016/j.envres.2021.111001.
[38] M.J. Lv, T. Zhang, H.B. Ya, Y. Xing, X. Wang, B. Jiang, Effects of heavy metals on the adsorption of ciprofloxacin on polyethylene microplastics: mechanism and toxicity evaluation, Chemosphere 315 (2023) 137745, https://doi.org/10.1016/j.chemosphere.2023.137745.
[39] Z. Chen, J. Fang, W. Wei, H.H. Ngo, W. Guo, B.-J. Ni, Emerging adsorbents for micro/nanoplastics removal from contaminated water: advances and perspectives, J. Clean. Prod. 371 (2022) 133676, https://doi.org/10.1016/j.jclepro.2022.133676.
[40] G.C. Assis, R. Antonelli, A.O.S. Dantas, A.C.S.C. Teixeira, Microplastics as hazardous pollutants: occurrence, effects, removal and mitigation by using plastic waste as adsorbents and supports for photocatalysts, J. Environ. Chem. Eng. 11 (6) (2023) 111107, https://doi.org/10.1016/j.jece.2023.111107.
[41] S. Ghosh, J.K. Sinha, S. Ghosh, K. Vashisth, S. Han, R. Bhaskar, Microplastics as an emerging threat to the global environment and human health, Sustainability 15 (2023) 10821, https://doi.org/10.3390/su151410821.
[42] M. Bahrami, M.J. Amiri, M.R. Mahmoudi, A. Zare, Statistical and mathematical modeling for predicting caffeine removal from aqueous media by rice husk-derived activated carbon, Sustainability 15 (9) (2023) 7366, https://doi.org/10.3390/su15097366.
[43] M.J. Amiri, J. Abedi-Koupai, S. Eslamian, S.F. Mousavi, M. Arshadi, Modelling Pb (II) adsorption based on synthetic and industrial wastewaters by ostrich bone char using artificial neural network and multivariate non-linear regression, Int. J. Hydrol. Sci. Technol. 3 (3) (2013) 221–240, https://doi.org/10.1504/IJHST.2013.058313.
[44] M.J. Amiri, R. Roohi, M. Arshadi, A. Abbaspourrad, 2,4-D adsorption from agricultural subsurface drainage by canola stalk-derived activated carbon: insight into the adsorption kinetics models under batch and column conditions, Environ. Sci. Pollut. Res. 27 (14) (2020) 16983–16997, https://doi.org/10.1007/s11356-020-08211-7.
[45] B. Beigzadeh, M. Bahrami, M.J. Amiri, M.R. Mahmoudi, A new approach in adsorption modeling using random forest regression, Bayesian multiple linear regression, and multiple linear regression: 2, 4-D adsorption by a green adsorbent, Water Sci. Technol. 82 (8) (2020) 1586–1602, https://doi.org/10.2166/wst.2020.440.
[46] M.J. Amiri, M. Bahrami, R. Rajabi, Assessment of M5 model tree for prediction of azithromycin antibiotic removal by multi-wall carbon nanotubes in a fixed-bed column system, Aqua Water Infrastruct. Ecosyst. Soc. 71 (4) (2022) 533–545, https://doi.org/10.2166/aqua.2022.157.
[47] B. Xu, F. Liu, P.C. Brookes, J. Xu, The sorption kinetics and isotherms of sulfamethoxazole with polyethylene microplastics, Mar. Pollut. Bull. 131 (2018) 191–196, https://doi.org/10.1016/j.marpolbul.2018.04.027.
[48] Saruchi, V. Kumar, Adsorption kinetics and isotherms for the removal of rhodamine B dye and Pb2+ ions from aqueous solutions by a hybrid ion-exchanger, Arab. J. Chem. 12 (2019) 316–329, https://doi.org/10.1016/j.arabjc.2016.11.009.
[49] M.J.D. Low, Kinetics of chemisorption of gases on solids, Chem. Rev. 60 (1960) 267–312, https://doi.org/10.1021/cr60205a003.
[50] M. Bahrami, M.J. Amiri, Nitrate removal from contaminated waters using modified rice husk ash by Hexadecyltrimethylammonium bromide surfactant, React. Kinet. Mech. Catal. 135 (2022) 459–478, https://doi.org/10.1007/s11144-021-02149-8.
[51] M. Bahrami, M.J. Amiri, S. Koochaki, Removal of caffeine from aqueous solution using multiwall carbon nanotubes: kinetic, isotherm, and thermodynamics studies, Pollution 3 (2017) 539–552, https://doi.org/10.22059/poll.2017.62771.
[52] L. Wang, Z.-P. Liu, X.-S. Zhang, L. Chen, Prediction of hot spots in protein interfaces using a random forest model with hybrid features, Protein Eng. Des. Sel. 25 (3) (2012) 119–126, https://doi.org/10.1093/protein/gzr066.
[53] A.J. Sage, Y. Liu, J. Sato, From black box to shining spotlight: using random forest prediction intervals to illuminate the impact of assumptions in linear regression, Am. Stat. 76 (2022) 414–429, https://doi.org/10.1080/00031305.2022.2107568.
[54] P.F. Smith, S. Ganesh, P. Liu, A comparison of random forest regression and multiple linear regression for prediction in neuroscience, J. Neurosci. Methods 220 (1) (2013) 85–91, https://doi.org/10.1016/j.jneumeth.2013.08.024.
[55] A. Benmessaoud, D. Nibou, E.H. Mekatel, S. Amokrane, A comparative study of the linear and non-linear methods for determination of the optimum equilibrium isotherm for adsorption of Pb^{2+} ions onto Algerian treated clay Iran. J. Chem. Chem. Eng. 39 (4) (2020) 153–171, https://doi.org/10.30492/ijcce.2019.35116.
[56] R. Ashkenazy, L. Gottlieb, S. Yannai, Characterization of acetone-washed yeast biomass functional groups involved in lead biosorption, Biotechnol. Bioeng. 55 (1997) 1–10, https://doi.org/10.1002/(SICI)1097-0290(19970705)55:1.
[57] J. Charles, G.R. Ramkumaar, S. Azhagiri, S. Gunasekaran, FTIR and thermal studies on nylon-66 and 30% glass fiber reinforced nylon-66, J. Chem. 6 (2009) 909017, https://doi.org/10.1155/2009/909017.
[58] F. Farrokhpey, E. Mofarah, R. Nik Khasal, Introduction to surface analyzes based on physical adsorption and desorption, Iran. J. Lab. Knowl. (IJLK) 6 (4) (2019) 7–12. ⟨https://sid.ir/paper/730533/en⟩.
[59] J.J. Salazar-Rabago, R. Leyva-Ramos, J. Rivera-Utrilla, R. Ocampo-Perez, F. J. Cerino-Cordova, Biosorption mechanism of Methylene Blue from aqueous

solution onto white pine (Pinus durangensis) sawdust: effect of operating conditions, Sustain. Environ. Res. 27 (2017) 32–40, https://doi.org/10.1016/j.serj.2016.11.009.
[60] B.H. Hameed, A.L. Ahmad, K.N.A. Latiff, Adsorption of basic dye (methylene blue) onto activated carbon prepared from rattan sawdust, Dyes Pigm 75 (2007) 143–149, https://doi.org/10.1016/j.dyepig.2006.05.039.
[61] S. Basu, G. Ghosh, S. Saha, Adsorption characteristics of phosphoric acid-induced activation of bio-carbon: equilibrium, kinetics, thermodynamics and batch adsorber design, Process Saf. Environ. Prot. 117 (2018) 125–142, https://doi.org/10.1016/j.psep.2018.04.015.
[62] J.R. Guarın, J.C. Moreno-Pirajan, L. Giraldo, Kinetic study of the bioadsorption of methylene blue on the surface of the biomass obtained from the algae *D. antarctica*, J. Chem. 2018 (2018) 2124845, https://doi.org/10.1155/2018/2124845.
[63] H. Zhang, S. Pap, M.A. Taggart, K.G. Boyd, N.A. James, S.W. Gibb, A review of the potential utilisation of plastic waste as adsorbent for removal of hazardous priority contaminants from aqueous environments, Environ. Pollut. 258 (2020) 113698, https://doi.org/10.1016/j.envpol.2019.113698.
[64] N.S. Awwad, A.A. El-Zahhar, J.A.M. Alasmary, Removal of methylene blue dyes from aqueous system using composite polymeric-apatite resins, In Chemistry and Technology of Natural and Synthetic Dyes and Pigments, Edited by A.K. Samanta, N.S. Awwad, H.M. Algarni, (pp. 1-13). IntechOpen, 10.5772/intechopen.92048.
[65] O.J. Redlich, D.L. Peterson, A useful adsorption isotherm, J. Phys. Chem. 63 (6) (1959) 1024, https://doi.org/10.1021/j150576a611.
[66] C. Lin, S. Li, M. Chen, R. Jiang, Removal of congo red dye by gemini surfactant C12-4-C12. 2Br-modified chitosan hydrogel beads, J. Dispers. Sci. Technol. 38 (2017) 46–57, https://doi.org/10.1080/01932691.2016.1138229.
[67] H. Chen, A. Wang, Adsorption characteristics of Cu(II) from aqueous solution onto poly(acrylamide)/attapulgite composite, J. Hazard. Mater. 165 (2009) 223–231, https://doi.org/10.1016/j.jhazmat.2008.09.097.
[68] D. Ozdes, A. Gundogdu, B. Kemer, C. Duran, H.B. Senturk, M. Soylak, Removal of Pb (II) ions from aqueous solution by a waste mud from copper mine industry: equilibrium, kinetic and thermodynamic study, J. Hazard. Mater. 166 (2009) 1480–1487, https://doi.org/10.1016/j.jhazmat.2008.12.073.
[69] M. Khormaei, B. Nasernejad, M. Edrisi, T. Eslamzadeh, Copper biosorption from aqueous solutions by sour orange residue, J. Hazard. Mater. 149 (2007) 269–274, https://doi.org/10.1016/j.jhazmat.2007.03.074.
[70] H.T. Kara, S.T. Anshebo, F.K. Sabir, G.A. Workineh, Removal of methylene blue dye from wastewater using periodiated modified nanocellulose, Int. J. Chem. Eng. 2021 (2021) 9965452, https://doi.org/10.1155/2021/9965452.
[71] L. Liu, H. Ma, B. Xing, Aging and characterization of disposable polypropylene plastic cups based microplastics and its adsorption for methylene blue, Chemosphere 349 (2024) 140976, https://doi.org/10.1016/j.chemosphere.2023.140976.
[72] J. Liu, Y. Ma, D. Zhu, T. Xia, Y. Qi, Y. Yao, X. Guo, R. Ji, W. Chen, Polystyrene nanoplastics-enhanced contaminant transport: role of irreversible adsorption in glassy polymeric domain, Environ. Sci. Technol. 52 (2018) 2677–2685, https://doi.org/10.1021/acs.est.7b05211.
[73] S.M. Hosseini, H. Younesi, R. Vajdi, N. Bahramifar, Selective adsorption of mercury (II) from aqueous solution using functionalized nanochitosan by carbon disulfide, Journal of Water and Wastewater, 31 (2) 57-75, dx.doi.org/10.22093/wwj.2019.187010.2870.